arXiv:1704.00738v1 [cond-mat.dis-nn] 3 Apr 2017

# Many-body Localization Transition: Schmidt Gap, Entanglement Length & Scaling

Johnnie Gray,[1] Sougato Bose,[1] and Abolfazl Bayat[1]

[1]*Department of Physics and Astronomy, University College London, Gower Street, London WC1E 6BT, United Kingdom**

(Dated: April 5, 2017)

Many-body localization has become an important phenomenon for illuminating a potential rift between non-equilibrium quantum systems and statistical mechanics. However, the nature of the transition between ergodic and localized phases in models displaying many-body localization is not yet well understood. Assuming that this is a continuous transition, analytic results show that the length scale should diverge with a critical exponent $\nu \geq 2$ in one dimensional systems. Interestingly, this is in stark contrast with all exact numerical studies which find $\nu \sim 1$. We introduce the Schmidt gap, new in this context, which scales near the transition with a exponent $\nu > 2$ compatible with the analytical bound. We attribute this to an insensitivity to certain finite size fluctuations, which remain significant in other quantities at the sizes accessible to exact numerical methods. Additionally, we find that a physical manifestation of the diverging length scale is apparent in the entanglement length computed using the logarithmic negativity between disjoint blocks.

*Introduction.–* In recent years, it has become apparent that the Anderson Localization [1] of disordered models can survive in the presence of interactions [2], with rigorous proof now found for one-dimensional systems [3]. This phenomena, known as many-body localization (MBL), has attracted much interest [4–9] in fundamental physics due to the fact that such systems generically break ergodicity and fail to thermalise — thus lying beyond the scope of statistical mechanics. Additionally, MBL occurs throughout the energy spectrum, implying that its fingerprint can be observed at all temperatures. These facts combined have significant practical implications for quantum transport [2] and information storage [10–12]. Experimental advances have allowed the controlled observation of MBL phenomena [13, 14], further driving interest.

Considerable progress has been made in understanding the strongly localized phase, particularly in terms of local integrables of motion [6, 15–18] , which permit a MPS description of all eigenstates [19–24]. However, eigenstates in the ergodic phase generally have volume law entanglement, restricting one to exact diagonalization techniques and small system sizes (up to $\sim 20$ spins) — this has constrained the development of a clear picture of the nature of the transition from ergodic to MBL (the MBLT). For example, questions that still require attention include: (i) Which quantities can best characterize the transition? (ii) Is it valid to treat the MBLT using the same framework, based on the emergence of a diverging length-scale, developed for zero-temperature quantum phase transitions? (iii) If so, what is the universal critical exponent, $\nu$, governing this length-scale? And (iv) what is the physical picture of the said length-scale?

An extensive exact numerical analysis of the MBLT, using a variety of quantities, can be found in [25], in which finite size scaling analysis throughout the spectrum allows the observation of a mobility edge. In fact, it is now commonplace to diagnose the MBLT with the mean energy level statistics and the block entanglement entropy [5, 9, 25–28]. These works are largely based on the assumption that the MBLT is continuous, and their exact numerical analyses have consistently found $\nu \sim 1$. This is in striking contrast with analytic results, found by Chayes-Chayes-Fisher-Spencer [29] and Chandran-Laumann-Oganesyan [30], which would demand $\nu \geq 2/d$ for system dimension $d$ (the CCFS/CLO bound). A recent explanation [28] posits that at the finite system sizes available for exact studies, the fluctuations in these quantities are not yet dominated by the true disorder. Thus it is highly desirable to use a new quantity better able to capture the real disorder induced transition properties.

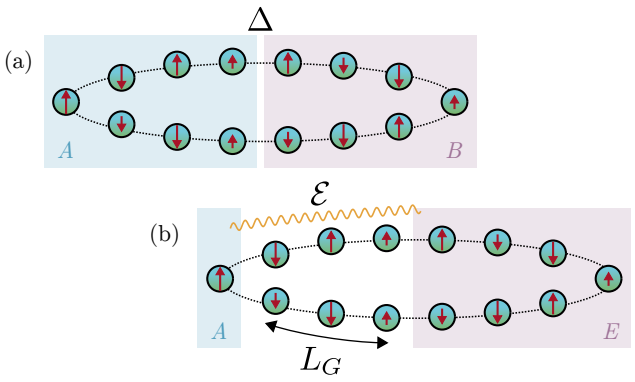


FIG. 1: Schematic of the two main quantities studied here: a) the Schmidt gap, $\Delta$, across a bipartition of the system and b) the logarithmic negativity, $\mathcal{E}$, between disjoint blocks separated by length $L_G$.

In this letter, we bring in new tools to understand the nature of the MBLT. Firstly, the Schmidt gap, which has been successfully employed as an order parameter in zero temperature quantum phase transitions [31–33]. Secondly, an entanglement length computed from the logarithmic negativity [34–38], quantifying the bipartite entanglement between two disjoint blocks [39–43], which

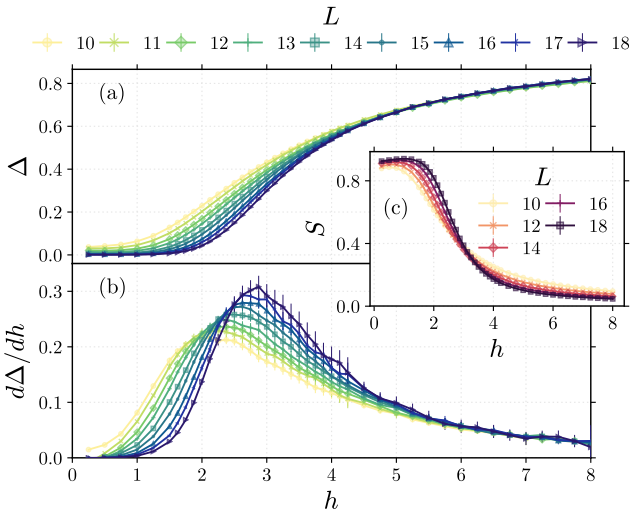


FIG. 2: (Color online) (a) and (b) : The Schmidt gap, $\Delta$, and its derivative as a function of disorder, $h$, across the MBLT for varying chain length, $L$. (c) The normalized half chain entropy, $S$, as a function of disorder for varying $L$.

has been previously used to probe the extension of the Kondo screening cloud [44, 45]. We find that, unlike previously used quantities, the Schmidt gap reveals a critical exponent $\nu \geq 2$, consistent with the CCFS/CLO bound. Moreover, we find that the entanglement length witnesses the emergence of a diverging length scale at the transition from ergodic to MBL phase.

*Model.–* We consider a periodic spin-1/2 Heisenberg chain, with random per site magnetic fields in the $z$-direction:

$$H = J \sum_{i=1}^{L} \left( \boldsymbol{S}_i \cdot \boldsymbol{S}_{i+1} - h_i S_i^z \right), \tag{1}$$

where $J$ is the exchange coupling, $\boldsymbol{S}_i = \frac{1}{2}(\sigma_i^x, \sigma_i^y, \sigma_i^z)$ describes a vector of Pauli matrices acting on spin $i$ and dimensionless parameter $h_i$ is the random magnetic field at site $i$ drawn from the flat distribution $[-h, h]$. This model conserves total $z$-spin, and we diagonalize in either the spin-0 or spin-$\frac{1}{2}$ subspaces for even and odd $L$ respectively. For each random instance of this Hamiltonian, we extract a number of eigenvectors, $\{|E_k\rangle\}$, in the middle of the energy spectrum [46, 47]. Since there is evidence of a mobility edge in MBL [25], at least for finite sizes, this targeting sharpens any transition observed. Unless stated, for each run any quantities calculated are averaged over 50 states around this energy, with errors ascribed based on the variance between samples of $H$.

*Characterizing the MBLT.–* The main quantity we compute, which has not been used in the context of MBL before, is the Schmidt gap. For two chain halves (or as close to for odd $L$), $A$ and $B$, as shown in Fig. 1(a), an eigenvector's reduced density matrix is $\rho_{A,k} = \mathrm{Tr}_B(|E_k\rangle \langle E_k|)$. The Schmidt gap is then defined as $\Delta = \langle \lambda_1^k - \lambda_2^k \rangle_k$, where $\lambda_1^k$, $\lambda_2^k$ refer to the largest eigenvalues of the reduced density matrix $\rho_{A,k}$. Previously, the Schmidt gap has been shown to act as an order parameter and capture quantum phase transitions in the ground state of zero temperature systems [31, 33]. We explore the possibility of using this quantity for characterizing the MBLT. Unlike entanglement entropy, the Schmidt gap uses only a fraction of the spectrum of $\rho_{A,k}$ and thus describes the relationship between only the two dominant states across the $A-B$ cut. In the ergodic phase we expect strong entanglement to produce multiple, equally likely orthogonal states, thus $\Delta \sim 0$. In the MBL phase, however, a single dominant state should appear on either side of the cut, with $\Delta$ eventually rising to 1 at $h = \infty$, implying a pure tensor product. This behaviour is shown in Fig. 2(a) and becomes becomes sharper with increasing $L$. To see this more vividly, we plot the derivative of $\Delta$ with respect to $h$ in Fig. 2(b). The derivative has a peak which not only becomes more pronounced but also shifts to the right with $L$. This suggests that in the thermodynamic limit, $L \to \infty$, the derivative of the Schmidt gap diverges at the MBLT and the peaks asymptotically approach the transition point $h_c$.

For reference, we consider the normalised half chain entropy, widely employed to herald the MBLT [5, 9, 25–28]. The von Neumann entropy of subsystem $A$ is defined as $S_{\mathrm{vn}} = -\mathrm{Tr}(\rho_{A,k} \log \rho_{A,k})$. This is normalized by the Page entropy [48], $S_P = (1/\log 2) \sum_{i=n+1}^{mn} \frac{1}{i} - \frac{m-1}{2n}$, with $m$, $n$ the Hilbert space dimensions of subsystems $A$ and $B$, yielding $S = \frac{\langle S_{\mathrm{vn}} \rangle_k}{S_P}$. $S_P$ is the expected entropy for a subsystem of a random pure state; since these overwhelmingly have entropy that scales as their enclosed volume, $S$ gives a measure of how far $|E_k\rangle$ has departed towards area law behaviour. In Fig. 2(c) the behaviour of $S$ across the MBLT is shown. In the ergodic phase its value approaches 1 (showing the volume law), whereas in the MBL phase it falls to 0 (representing the area law), as expected.

*Scaling.–* The behaviour observed in Figs. 2(a)-(b) suggests that the MBLT is a continuous transition in which a diverging length scale $\xi \propto |h - h_c|^{-\nu}$ emerges near the transition point, consistent with previous studies [9]. In order to estimate the exponent $\nu$, finite size scaling analysis [49] has previously been employed for various quantities, including the entanglement entropy $S$. These analyses, based on exact numerical methods, find $\nu \sim 1$ [25, 28, 50], contradicting the CCFS/CLO bound. A recently proposed explanation [28], suggests that there are two universality classes at play here, one dominated by intrinsic intra-sample randomness between eigenstates, the second by inter-sample randomness between field configurations — with this second class growing but not yet dominant for system sizes studied. However, for a *quasiperiodic* (QP) model, where the field $h_i$ is given by $\cos(2\pi\beta i - \delta)$, with $\beta$ an irrational number such

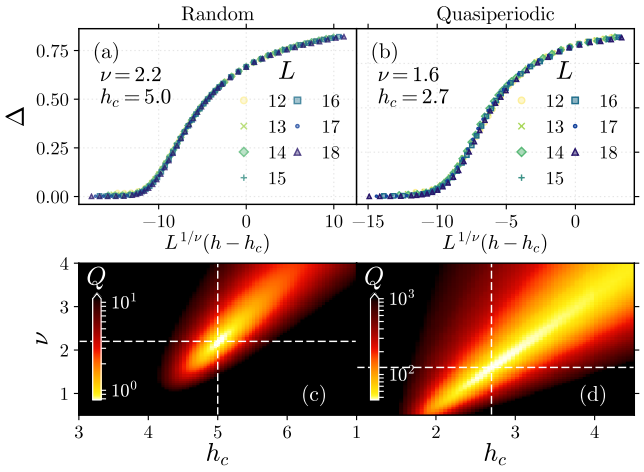


FIG. 3: (Color online) (a) and (b): Schmidt gap data collapse for the random and quasiperiodic model respectively with fitting parameters as shown. (c) and (d): Quality of data collapse, $Q$, (lower is better) across the whole parameter space for the random and quasiperiodic models respectively. The dashed lines denote the minimum points with which (a) and (b) are plotted.

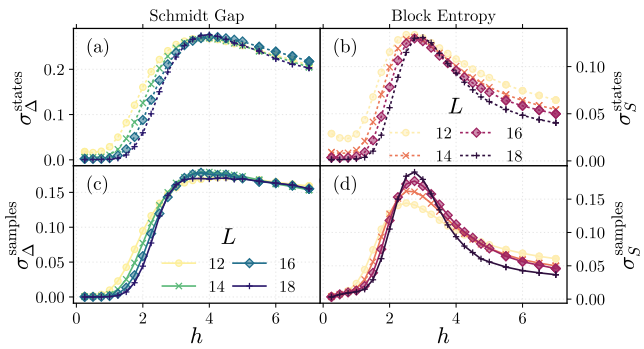


FIG. 4: (Color online) (a) and (b): Standard deviation between eigenstates across the MBLT for the Schmidt gap and normalized block entropy respectively. (c) and (d): Standard deviation between samples across the MBLT for the Schmidt gap and normalized block entropy respectively.

that the field is incommensurate with the lattice and $\delta$ a random offset, any sample to sample variance (by varying $\delta$ only) must vanish in the thermodynamic limit, and a separate constraint, $\nu > 1/d$, is relevant [51]. In [28] they find that $\nu$ for a QP model is smaller but close ($\sim 1$) to that of a random model for reachable system sizes, reasoning that both models are showing scaling dominated by the intra-sample universality class.

In order to estimate the exponent $\nu$ for both models, using the Schmidt gap, we consider the following finite size scaling ansatz,

$$\Delta = f(L^{1/\nu}(h - h_c)), \tag{2}$$

where $f(.)$ is an unspecified function. In Fig. 3(a) and (b) we show optimal data collapse of $\Delta$ for the random and QP distributions of $h_i$ respectively. So as to sample faithfully from the $L \to \infty$ QP model, we take open boundary conditions. For the random model, we find $\nu = 2.2$, in agreement with the CCFS/CLO bound. For the quasiperiodic model however, we find $\nu = 1.6$ — significantly lower than the random case, but in agreement with its respective bound, i.e. $\nu \geq 1/d$ [51]. In order to give a sense of the leeway available when fitting the data, in Fig. 3(c) and (d) we plot the quality of collapse, $Q$, calculated using the method refined in [52], as a function of the critical parameters. In both the random and QP case, we see that there is considerable correlation between the optimum $\nu$ and $h_c$. This increases the difficulty in ascribing independent errors, and means that lower values of $\nu$ fit best with lower values of $h_c$. By comparing Fig. 2(a) and (c), we note that the pronounced intersection of the different length curves for the block entropy is not apparent in the Schmidt gap. Thus, one might conjecture an ansatz different from that of Eq. (2). This new ansatz, $\Delta \sim L^{-\beta/\nu} f(L^{1/\nu}(h - h_c))$, considers an extra exponent $\beta$ and assumes behaviour like an order parameter for the Schmidt gap — in the thermodynamic limit it would remain zero throughout the ergodic phase and suddenly rise at the transition point according to $\Delta \sim |h - h_c|^\beta$. The finite sizes used here do not allow us pinpoint $\beta$, other than it would have to be $0 \leq \beta \leq 0.1$, and thus distinguish these two ansatz. A more detailed discussion of this issue is presented in the supplementary material.

*Schmidt gap vs. entanglement entropy.–* In order to understand why the Schmidt gap is more successful than typical quantities, such as entanglement entropy, we study the deviation of $\Delta$ and $S$ in the random model. Similar to Ref. [28], we define two different types of spread for both the Schmidt gap, $\Delta$, and the normalized block entropy, $S$: (i) the standard deviation between eigenvectors in a single sample, then averaged over samples — $\sigma_\Delta^{\text{states}}$ and $\sigma_S^{\text{states}}$; and (ii) the standard deviation between samples, once each quantity has been averaged over eigenstates — $\sigma_\Delta^{\text{samples}}$ and $\sigma_S^{\text{samples}}$. Both the Schmidt gap and the normalized block entropy must lie between 0 and 1, thus their standard deviation is capped as 0.5. In Fig. 4(a) and (b) we plot $\sigma_\Delta^{\text{states}}$ and $\sigma_S^{\text{states}}$ as functions of $h$ for various system sizes. It can be seen that for both cases, the peak value is constant with $L$, suggesting that the effect of inter-state randomness has saturated. The situation is different for $\sigma_\Delta^{\text{samples}}$ and $\sigma_S^{\text{samples}}$, as shown in Fig. 4(c) and (d). While $\sigma_\Delta^{\text{samples}}$ is saturated, $\sigma_S^{\text{samples}}$ is still growing with $L$. This suggests that the effect of the true disorder on $S$ has yet to saturate, with each $L$ feeling a different strength. We thus conclude that the Schmidt gap is less sensitive to the finite size effects. A likely explanation is that $\Delta$ ignores the exponentially growing number of Schmidt coefficients — which may be susceptible to many fluctuations — and

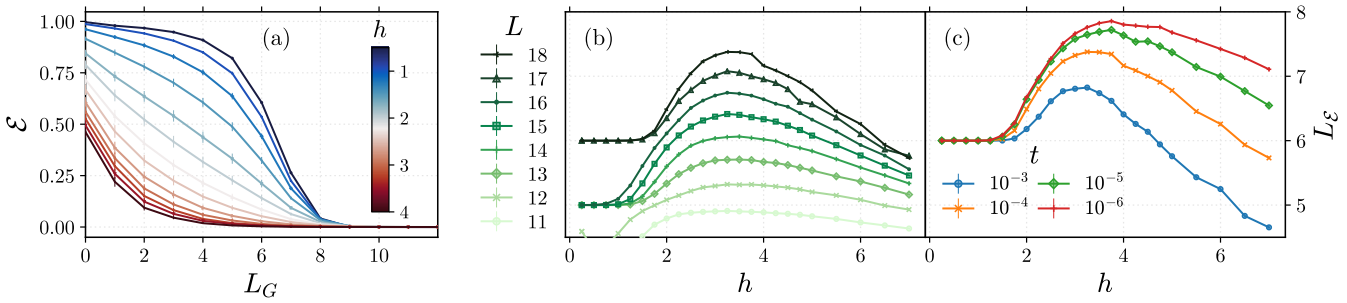


FIG. 5: (Color online) (a) Average logarithmic negativity as a function of the gap between two disjoint blocks, the first block being a single spin, the second the rest of the system as depicted in Fig. 1(b), for $L = 14$, which has a pseudo-critical point at $h \sim 2$. (b) Entanglement length, $L_\mathcal{E}$ as a function of disorder for varying chain length, here with threshold $t = 10^{-4}$. (c) The same, but now for varying threshold $t$, with the length set at $L = 18$.

queries only the dominant behaviour.

*Entanglement length.–* The nature of the diverging length scale $\xi$, in the context of MBLT, is mysterious and a physical picture is lacking. To shed light on this, we introduce an entanglement length, as previously used for detecting the Kondo screening cloud [44, 45]. Specifically, we consider the entanglement between a small subsystem $A$, here a single spin, and an environment $E$, separated by a gap of length $L_G$, a geometry shown in Fig. 1(b). The reduced state of the two blocks is $\rho_{AE,k} = \mathrm{Tr}_G(|E_k\rangle\langle E_k|)$. We use the logarithmic negativity [34–38] to quantify the entanglement between systems $A$ and $E$, defining $\mathcal{E}(L_G) = \left\langle \log ||\rho^\Gamma_{AE,k}||_1 \right\rangle_k$, with $\Gamma$ the partial transpose, and $||\cdot||_1$ the trace norm. In the ergodic phase, due to volume law entanglement, the eigenstates are highly multipartite entangled between their spins and thus $\mathcal{E}(L_G)$ is expected to decay slowly with increasing $L_G$. In the MBL phase, however, $A$ will be weakly entangled with only spins close to it, and thus $\mathcal{E}(L_G)$ should decay quickly. In Fig. 5(a) we plot $\mathcal{E}$ as a function of $L_G$ for various disorder strengths $h$ in an open chain of length $L = 14$. The choice of an open chain here is simply to have larger values of $L_G$ and similar results are found in periodic chains. As is clear from the figure, in the ergodic phase $\mathcal{E}$ decays very slowly as opposed to its fast exponential decay in the MBL phase. At the pseudo-critical point, $h \sim 2$ for $L = 14$, entanglement decays close to linearly — each spin lost contributes equally to the entanglement. This fits with a picture of a self-similar structure of entangled clusters [27, 53]. To extract a length scale from $\mathcal{E}(L_g)$ we look at the behaviour of its tail, and query at what point it drops below a certain small threshold value, $t$, of its initial value. In this way we define an entanglement length $L_\mathcal{E} = \min\{L_G : \mathcal{E}(L_G) < t\mathcal{E}(0)\}$. The behaviour of this is shown in Fig. 5(b), in which it can be seen to peak for each $L$ across the critical region, – evidence that the diverging length scale $\xi$ leaves its fingerprint on both sides of the transition. A plausible explanation for the *increase* in $L_\mathcal{E}$ as one approaches the MBLT from the ergodic side is that proximal spins become off-resonant so that bonding (bipartite entanglement) takes place at increasingly longer scales. A similar technique, but using the mutual information [54], does not recover a peak at the transition, demonstrating that focusing on only quantum correlations can reveal quite different behaviour. For completeness, the effect of varying the threshold required, $t$, is shown in Fig. 5(c) — there is only a slight drift when changing the threshold. An alternative approach to identifying the diverging length scale on the ergodic side based on the entanglement spectrum has been recently developed in Ref. [55]. It is an interesting open question whether that length is related to the entanglement length proposed here.

*Conclusions.–* In this letter we have explored the MBLT using the Schmidt gap and the entanglement length. We show that the Schmidt gap not only exhibits scaling at the MBLT, but does so with a critical exponent $\nu > 2$, compatible with analytic predictions. This compatibility is absent in all quantities studied with exact numerical methods thus far, a fact that we attribute to the presence of significant finite size fluctuations which the Schmidt gap is less sensitive to. We have also considered an entanglement length computed using the logarithmic negativity across two disjoint blocks, which peaks at the transition point. This yields a physical picture of the emergence of a diverging length scale at the MBLT. Our investigations open several questions, including: (i) whether the Schmidt gap might behave as an order parameter, displaying non-analytic behaviour in its derivative at the MBLT; and (ii) whether the entanglement length identified by us has any manifestation in the multipartite entanglement as one approaches the MBLT.

*Acknowledgements.–* JG acknowledges funding from the EPSRC Center for Doctoral Training in Delivering Quantum Technologies at UCL. AB and SB acknowledge the EPSRC grant EP/K004077/1. SB acknowledges financial support by the ERC under Starting Grant 308253 PACOMANEDIA.

* Electronic address: john.gray.14@ucl.ac.uk


[1] P. W. Anderson, Phys. Rev. **109**, 1492 (1958).
[2] D. M. Basko, I. L. Aleiner, and B. L. Altshuler, Ann. Phys. **321**, 1126 (2006), ISSN 0003-4916.
[3] J. Z. Imbrie, Phys. Rev. Lett. **117**, 027201 (2016).
[4] D. J. Luitz and Y. B. Lev, arXiv:1610.08993 [cond-mat] (2016), 1610.08993.
[5] R. Nandkishore and D. A. Huse, Annu. Rev. Condens. Matter Phys. **6**, 15 (2015).
[6] D. A. Huse, R. Nandkishore, and V. Oganesyan, Phys. Rev. B **90**, 174202 (2014).
[7] R. Sims and G. Stolz, arXiv:1312.0577 [math-ph] (2013), 1312.0577.
[8] J. H. Bardarson, F. Pollmann, and J. E. Moore, Phys. Rev. Lett. **109**, 017202 (2012).
[9] A. Pal and D. A. Huse, Phys. Rev. B **82**, 174411 (2010).
[10] N. Y. Yao, C. R. Laumann, and A. Vishwanath, arXiv:1508.06995 [cond-mat, physics:quant-ph] (2015), 1508.06995.
[11] R. Vasseur, S. A. Parameswaran, and J. E. Moore, Phys. Rev. B **91**, 140202 (2015).
[12] M. Serbyn, M. Knap, S. Gopalakrishnan, Z. Papić, N. Y. Yao, C. R. Laumann, D. A. Abanin, M. D. Lukin, and E. A. Demler, Phys. Rev. Lett. **113**, 147204 (2014).
[13] M. Schreiber, S. S. Hodgman, P. Bordia, H. P. Lüschen, M. H. Fischer, R. Vosk, E. Altman, U. Schneider, and I. Bloch, Science **349**, 842 (2015), ISSN 0036-8075, 1095-9203.
[14] J. Smith, A. Lee, P. Richerme, B. Neyenhuis, P. W. Hess, P. Hauke, M. Heyl, D. A. Huse, and C. Monroe, Nature Phys. **12**, 907 (2016), ISSN 1745-2473.
[15] R. Nandkishore, S. Gopalakrishnan, and D. A. Huse, Phys. Rev. B **90**, 064203 (2014).
[16] A. Chandran, I. H. Kim, G. Vidal, and D. A. Abanin, Phys. Rev. B **91**, 085425 (2015).
[17] V. Ros, M. Müller, and A. Scardicchio, Nucl. Phys. B **891**, 420 (2015), ISSN 0550-3213.
[18] C. Monthus, J. Stat. Mech. Theor. Exp **2016**, 033101 (2016), ISSN 1742-5468.
[19] M. Friesdorf, A. H. Werner, W. Brown, V. B. Scholz, and J. Eisert, Phys. Rev. Lett. **114**, 170505 (2015).
[20] M. Serbyn, A. A. Michailidis, D. A. Abanin, and Z. Papić, Phys. Rev. Lett. **117**, 160601 (2016).
[21] T. B. Wahl, A. Pal, and S. H. Simon, arXiv:1609.01552 [cond-mat, physics:quant-ph] (2016), 1609.01552.
[22] C. Zhang, F. Pollmann, S. L. Sondhi, and R. Moessner, arXiv:1608.06411 [cond-mat] (2016), 1608.06411.
[23] M. Žnidarič, Phys. Rev. Lett. **117** (2016).
[24] T. Devakul, V. Khemani, F. Pollmann, D. Huse, and S. Sondhi, arXiv:1702.07721 [cond-mat, physics:quant-ph] (2017), 1702.07721.
[25] D. J. Luitz, N. Laflorencie, and F. Alet, Phys. Rev. B **91**, 081103 (2015).
[26] P. Ponte, Z. Papić, F. Huveneers, and D. A. Abanin, Phys. Rev. Lett. **114**, 140401 (2015).
[27] V. Khemani, S. P. Lim, D. N. Sheng, and D. A. Huse, arXiv:1607.05756 [cond-mat] (2016), 1607.05756.
[28] V. Khemani, D. N. Sheng, and D. A. Huse, arXiv:1702.03932 [cond-mat] (2017), 1702.03932.
[29] J. T. Chayes, L. Chayes, D. S. Fisher, and T. Spencer, Phys. Rev. Lett. **57**, 2999 (1986).
[30] A. Chandran, C. R. Laumann, and V. Oganesyan, arXiv:1509.04285 [cond-mat] (2015), 1509.04285.
[31] G. De Chiara, L. Lepori, M. Lewenstein, and A. Sanpera, Phys. Rev. Lett. **109**, 237208 (2012).
[32] L. Lepori, G. De Chiara, and A. Sanpera, Phys. Rev. B **87**, 235107 (2013).
[33] A. Bayat, H. Johannesson, S. Bose, and P. Sodano, Nat. Commun. **5** (2014).
[34] A. Peres, Phys. Rev. Lett. **77**, 1413 (1996).
[35] M. Horodecki, P. Horodecki, and R. Horodecki, Phys. Lett. A **223**, 1 (1996), ISSN 0375-9601.
[36] J. Lee, M. S. Kim, Y. J. Park, and S. Lee, J. Mod. Opt. **47**, 2151 (2000), ISSN 0950-0340.
[37] G. Vidal, Phys. Rev. A **65** (2002).
[38] M. B. Plenio, Phys. Rev. Lett. **95** (2005).
[39] H. Wichterich, J. Molina-Vilaplana, and S. Bose, Phys. Rev. A **80**, 010304 (2009).
[40] H. Wichterich, J. Vidal, and S. Bose, Phys. Rev. A **81**, 032311 (2010).
[41] C. D. Nobili, A. Coser, and E. Tonni, J. Stat. Mech. Theor. Exp. **2015**, P06021 (2015), ISSN 1742-5468.
[42] A. Coser, E. Tonni, and P. Calabrese, J. Stat. Mech. Theor. Exp. **2016**, 033116 (2016), ISSN 1742-5468.
[43] A. Coser, E. Tonni, and P. Calabrese, J. Stat. Mech. Theor. Exp. **2016**, 053109 (2016), ISSN 1742-5468.
[44] A. Bayat, P. Sodano, and S. Bose, Phys. Rev. B **81**, 064429 (2010).
[45] A. Bayat, S. Bose, P. Sodano, and H. Johannesson, Phys. Rev. Lett. **109**, 066403 (2012).
[46] L. D. Dalcin, R. R. Paz, P. A. Kler, and A. Cosimo, Adv. Water Resour. **34**, 1124 (2011), ISSN 0309-1708.
[47] V. Hernandez, J. E. Roman, and V. Vidal, ACM Trans. Math. Softw. **31**, 351 (2005), ISSN 0098-3500.
[48] D. N. Page, Phys. Rev. Lett. **71**, 1291 (1993).
[49] M. E. Fisher and M. N. Barber, Phys. Rev. Lett. **28**, 1516 (1972).
[50] J. A. Kjäll, J. H. Bardarson, and F. Pollmann, Phys. Rev. Lett. **113**, 107204 (2014).
[51] J. M. Luck, EPL **24**, 359 (1993), ISSN 0295-5075.
[52] J. Houdayer and A. K. Hartmann, Phys. Rev. B **70**, 014418 (2004).
[53] A. C. Potter, R. Vasseur, and A. Parameswaran, S., Phys. Rev. X **5**, 031033 (2015).
[54] G. De Tomasi, S. Bera, J. H. Bardarson, and F. Pollmann, Phys. Rev. Lett. **118**, 016804 (2017).
[55] F. Pietracaprina, G. Parisi, A. Mariano, S. Pascazio, and A. Scardicchio, arXiv:1610.09316 [cond-mat, physics:quant-ph] (2016), 1610.09316.

## SUPPLEMENTARY MATERIAL

In this supplementary material, we present further details regarding the Schmidt gap, its scaling, and the disjoint logarithmic negativity entanglement length.

### Schmidt Coefficients

The Schmidt gap, $\Delta$, quantifies the competition between the two dominant states either side of a partition. For completeness, in Fig. S1 we show more detailed behaviour of many Schmidt coefficients, $\lambda_i$, across a bipartition. Here, $\lambda_1, \lambda_2 ... \lambda_m$ are the non-increasing eigenvalues of a half chain reduced density matrix, known as the entanglement spectrum or Schmidt coefficients, averaged over eigenstates and samples. Their value as a function of disorder for $n = 18$ is shown in Fig. S1. On the ergodic side, it can be seen that many states are equally likely, whereas on the localized side, a power-law like spectrum emerges [20] according to which all Schmidt coefficients decay except $\lambda_1$. The distinction in the behaviour of $\lambda_1$ with respect to all the other Schmidt coefficients justifies the particular definition of Schmidt gap using only the two largest $\lambda$'s. One attractive aspect of the Schmidt worth noting, is that if one is to partition the chain in non-equal parts, $\Delta$ is largely oblivious to this change apart until one block becomes smaller than $\sim 3$.

### Schmidt Gap as an Order Parameter

In other studies of the Schmidt gap for ground state criticality at zero temperature, it has been observed to behave as an order parameter [31, 32], even when there is no obvious symmetry breaking [33]. Taking a scaling of the form $\Delta \sim L^{-\beta/\nu} f(L^{1/\nu}(h - h_c))$, the non-order parameter case corresponds to $\beta = 0$. In this case and in the thermodynamic limit, $\Delta$ will smoothly rise from zero in the ergodic phase and goes to 1 in the deep MBL phase with a point of inflection exactly at $h = h_c$. In finite size systems, however, the scaling function $f$ is constant at the transition point and thus $\Delta$ must be constant for varying $L$, and a intersection of (unscaled) data for each $L$ will occur. This is clearly the case for quantities such as the half-chain block entropy, although the point of intersection clearly drifts, presumably due to finite size effects. Looking at the data for $\Delta$ however, there not a definite point of intersection, leaving the possibility open whether it could be an order parameter resulting in a non-zero exponent $\beta$. In this case, in the thermodynamic limit, it would remain 0 right until the transition point. To explore this possibility, we again compute the quality of fit for a range of $\nu$ and $h_c$ values, but for each we optimize $\beta$ to achieve the best quality fit. The best quality fit for both the random and quasiperiodic models is shown in Fig. S2(a) and (b) respectively, along with the fitting parameters $\nu$ and $h_c$. Notably, the random model still has a $\nu$ larger than the quasi-periodic model, but smaller than the $\beta = 0$ case. In Fig. S2(c) and (d), we show the spread of collapse quality. In both cases, the required $\beta$ is very

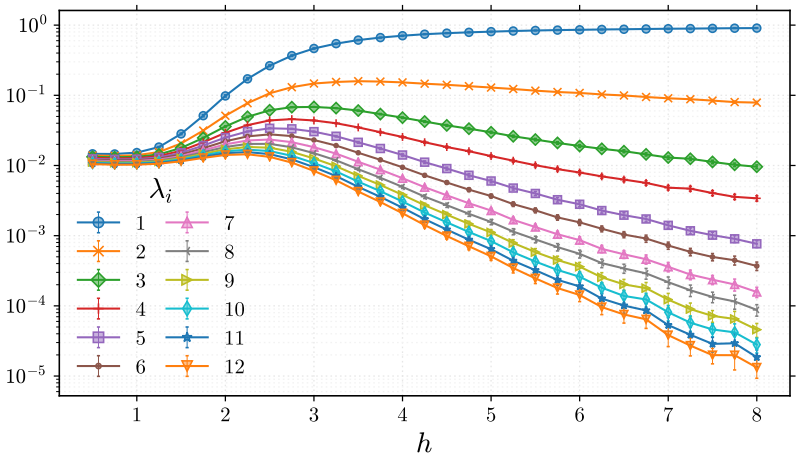


FIG. S1: (Color online) Value of the first 12 Schmidt coefficients $\lambda_i$ as a function of disorder $h$ across the MBLT, for $L = 18$. Error bars derived from sample variance are shown where visible.

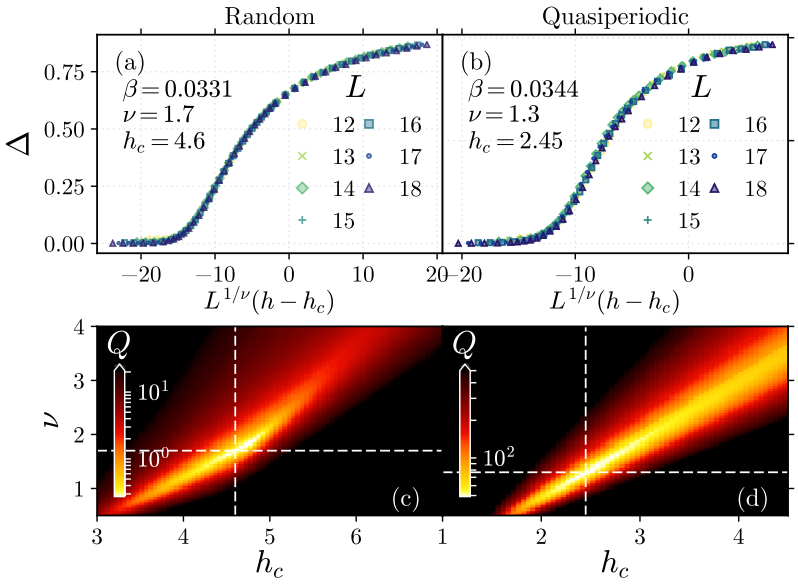


FIG. S2: (Color online) (a) and (b) Scaled Schmidt gap, $\Delta$, utilizing an optimized order parameter exponent, $\beta$, with best fit parameters shown. (c) and (d) Quality of fit (once $\beta$ has been optimized), for the two models, with dashed lines denoting the fitting parameters above.

small, however, the small system sizes that are available for exact diagonalization are not sufficient to confidently determine the exact value of $\beta$. From assessing the range of $\beta$ produced by various fitting parameters, we predict that the real value of the exponent would lie within the interval $0 \leq \beta \leq 0.1$.

### Disjoint Logarithmic Negativity for $L_A = 2$

Our entanglement length does not depend on the size of block $A$, which has been taken to be 1 in the paper. This is due to the fact that at the critical point $h_c$ we expect a self similar structure of entangled clusters to emerge. If we consider the logarithmic negativity between disjoint blocks, $\mathcal{E}(L_G)$, then we should find that the size of initial block chosen, $L_A$, (thus far 1 spin) has no qualitative effect on the results. In Fig. S3 we demonstrate this with $L_A = 2$ — apart from an overall factor of two the exact same features are visible for $\mathcal{E}$, and likewise for $L_\mathcal{E}(L)$ and $L_\mathcal{E}(t)$. As these figures show all the behaviour that we have found for $L_A = 1$ will remain valid for $L_A = 2$ as well.

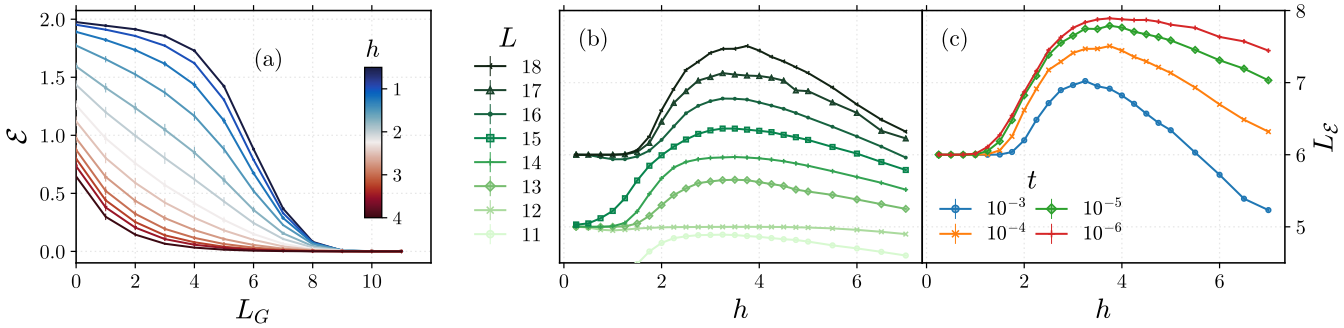


FIG. S3: (Color online) (a) Logarithmic negativity, $\mathcal{E}$, as a function of gap length between system $A$ of size $L_A = 2$ and the remaining environment, for varying disorder strength $h$. Here $L = 14$ and open boundary conditions are taken — such a model has an observed pseudo-critical point at $h \sim 2$. (b) Entanglement length $L_\mathcal{E}$ as a function of disorder for varying system lengths $L$ for $L_A = 2$. (c) The same, but for $L = 18$ and varying the threshold used to the define the entanglement length instead.